Ac susceptibility studies of multiferroic $BiMnO_3$ and solid solutions between $BiMnO_3$ and $BiScO_3$

2008 J. Phys.: Condens. Matter 20 025211

(http://iopscience.iop.org/0953-8984/20/2/025211)

J. Phys.: Condens. Matter **20** (2008) 025211 (6pp) doi:10.1088/0953-8984/20/02/025211

Ac susceptibility studies of multiferroic $BiMnO_3$ and solid solutions between $BiMnO_3$ and $BiScO_3$

Alexei A Belik[1] **and Eiji Takayama-Muromachi**

Advanced Nano Materials Laboratory (ANML), National Institute for Materials Science (NIMS), 1-1 Namiki, Tsukuba, Ibaraki 305-0044, Japan

E-mail: Alexei.BELIK@nims.go.jp

Received 9 July 2007, in final form 22 October 2007
Published 6 December 2007
Online at stacks.iop.org/JPhysCM/20/025211

Abstract

The real and imaginary parts of the ac susceptibilities of powder $BiMnO_3$ and $BiMn_{1-x}Sc_xO_3$ ($x = 0.1$, 0.2, 0.3, 0.4, 0.5, and 0.7) samples have been measured as functions of temperature, different driving ac and applied dc magnetic fields, and different ac magnetic field frequencies. Both χ' versus T and χ'' versus T showed strong dependence on the parameters of the ac magnetic field for ferromagnetic samples $BiMnO_3$ and $BiMn_{1-x}Sc_xO_3$ ($x = 0.1$, 0.2, and 0.3), indicating that the ac field interacted mainly with the domain structure. In $BiMn_{1-x}Sc_xO_3$ ($x = 0.1$, 0.2, and 0.3), a re-entrant spin-glass transition emerged at low temperatures. The re-entrant spin-glass transition temperature T_{RSG} increased with increasing x ($T_{RSG} = 4$ K for $x = 0.1$, $T_{RSG} = 5$ K for $x = 0.2$, and $T_{RSG} = 9$ K for $x = 0.3$). For $BiMn_{1-x}Sc_xO_3$ ($x = 0.4$, 0.5, and 0.7), only the classical spin-glass transition was found (the freezing temperature $T_f = 24$ K for $x = 0.4$, $T_f = 18$ K for $x = 0.5$, and $T_f = 7$ K for $x = 0.7$) with characteristic frequency dependence of broad maxima on the χ' versus T and χ'' versus T curves and no dependence on the driving ac field.

(Some figures in this article are in colour only in the electronic version)

1. Introduction

$BiMnO_3$ has recently attracted much interest as a multiferroic material because it has a robust ferromagnetism and possibly a ferroelectric state [1]. Evidence for a ferroelectric state in $BiMnO_3$ thin films was obtained from optical second-harmonic generation response [2] and writing polarization bits by a Kelvin force microscope [3]. Direct measurements of ferroelectric hysteresis loops were reported only in one work [4]. On the other hand, structural analysis of bulk $BiMnO_3$ using neutron powder diffraction [5, 6], convergent-beam electron diffraction [5], and first-principles calculations [7] suggested the centrosymmetric structure. Possible explanation of these contradictory results is the stain effect in thin films and the effect of stoichiometry [5, 7, 8].

Thin film samples of $BiMnO_3$ and slightly doped $Bi_{1-x}La_xMnO_3$ have shown promising results for practical applications [2, 3, 9–11]. $BiMnO_3$ orders ferromagnetically below $T_C = 99$–103 K [5, 12–14]. In addition, orbital degrees of freedom are also active in $BiMnO_3$ similar to $LaMnO_3$, as found by resonant x-ray scattering studies [15]. Therefore, different order parameters exist in $BiMnO_3$ and make it quite interesting. Recently, spin–glass-like behavior was observed in the magnetic properties of bulk and thin-film samples of $BiMnO_3$ [16, 17]. Specific heat data at low temperatures gave evidence for the presence of additional magnetic contributions in addition to the simple ferromagnetic spin-wave term [17].

We have recently investigated solid solutions between isostructural [5, 18] $BiMnO_3$ and $BiScO_3$ using specific heat, dc magnetization, differential scanning calorimetry, electron and x-ray diffraction [19, 20]. The zero-field-cooled (ZFC) dc magnetic susceptibilities of $BiMn_{1-x}Sc_xO_3$ with $x \geqslant 0.05$ showed the same features and were typical for ferromagnetic cluster–glass materials. However, in $BiMn_{0.6}Sc_{0.4}O_3$, evidence for the true spin-glass (SG) transition at the freezing temperature $T_f = 24$ K was found using the ac susceptibilities, namely, the typical frequency (f) shift of T_f ($\delta T_f = \Delta T_f / (T_f \Delta \log_{10} f) = 0.01$) and independence of the ac

[1] Author to whom any correspondence should be addressed.

susceptibilities on the driving ac field [19]. Specific heat and dc magnetization measurements could not distinguish the magnetic properties of $BiMn_{1-x}Sc_xO_3$ with $x \geqslant 0.05$. The specific heat anomaly near T_C in $BiMn_{1-x}Sc_xO_3$ with $x = 0.1$ and 0.2 was strongly suppressed compared with that of $BiMnO_3$, and no anomaly was found in $BiMn_{0.7}Sc_{0.3}O_3$. No principal difference was observed between the ZFC magnetic susceptibilities and the low-temperature specific heat of $BiMn_{0.7}Sc_{0.3}O_3$ and $BiMn_{0.5}Sc_{0.5}O_3$.

Ac susceptibility measurements can give more information about ground states of magnetic materials and the origin of magnetic anomalies. Therefore in this work, we performed detailed measurements of the real and imaginary components of the ac magnetic susceptibilities, depending on different driving ac (H_{ac}) and applied dc magnetic fields and different ac magnetic field frequencies (f) in $BiMnO_3$ and $BiMn_{1-x}Sc_xO_3$ ($x = 0.1$, 0.2, 0.3, 0.4, 0.5, and 0.7) focusing mainly on the H_{ac} and f dependences. We have found different magnetic behaviors of $BiMnO_3$, $BiMn_{1-x}Sc_xO_3$ with $x = 0.1$, 0.2, 0.3, and $BiMn_{1-x}Sc_xO_3$ with $x = 0.4$, 0.5, 0.7.

2. Experimental details

The synthesis of $BiMnO_3$ and $BiMn_{1-x}Sc_xO_3$ with $x = 0.05$, 0.1, 0.2, 0.3, 0.4, 0.5, and 0.7 is described in [5, 19]. Ac susceptibility measurements were performed with a Quantum Design MPMS instrument on cooling from 200 K at different frequencies ($f = 0.5$, 1.99, 7, 25, 99.9, 110, 299.5, and 997.3 Hz), applied oscillating magnetic fields ($H_{ac} =$ 0.01–5 Oe; 5 Oe is the maximum H_{ac} of our instrument), and static magnetic fields ($H_{dc} = 0.1$–5 kOe; at each H_{dc}, the measurements were taken from 200 to 2 K). Frequencies are expressed in round numbers below.

The time-dependent dc relaxation curves of $BiMn_{0.6}Sc_{0.4}O_3$ were measured at 100 Oe after cooling the sample from 150 K to the desired temperature at zero magnetic field (the waiting time before setting 100 Oe was 5 min). The relaxation curves were measured several times at each temperature to check the reproducibility. Good agreement between different measurements was observed. Another protocol for the relaxation measurements, namely, cooling in a magnetic field and measuring in zero magnetic field, was not used because there is always a small trapped magnetic field inside the superconducting magnet. This uncontrolled trapped field has a strong effect and considerably reduces the reproducibility. We have also investigated an aging phenomenon in $BiMn_{0.6}Sc_{0.4}O_3$ using the following procedure: the sample was cooled from 150 to 10 K at zero magnetic field and kept at 10 K for a wait-time ($t_w = 10^2$, 10^3, and 10^4 s); thereafter a dc field of 1 Oe was applied, and the magnetization was measured as a function of time.

3. Results

3.1. $BiMnO_3$

Figure 1 shows the χ' versus T and χ'' versus T curves of $BiMnO_3$ as a function of temperature at $f = 110$ Hz and

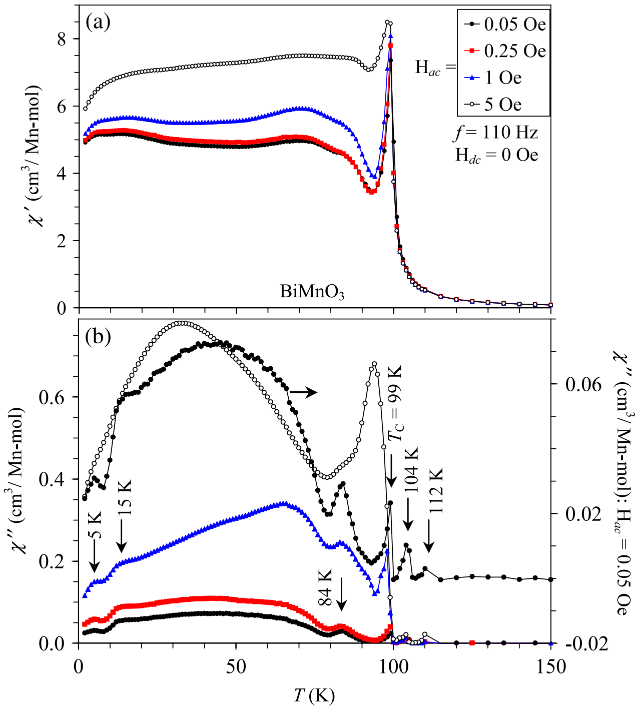

Figure 1. The real χ' (a) and imaginary χ'' (b) parts of the ac susceptibilities for $BiMnO_3$ as a function of temperature at the frequency $f = 110$ Hz, zero static magnetic field (H_{dc}), and different driving ac fields (H_{ac}). The secondary y axis in (b) gives the χ'' versus T curve at $H_{ac} = 0.05$ Oe. Vertical arrows are attached to the observed anomalies.

different ac magnetic fields varying from 0.05 to 5 Oe. There is a strong dependence of both components on H_{ac}. The magnetic losses at $H_{ac} = 5$ Oe are about one order of magnitude larger than those at $H_{ac} = 0.05$ Oe. The peak position near T_C on the χ'' versus T curves depends on H_{ac} (99 K for $H_{ac} = 0.05$ Oe and 94 K for $H_{ac} = 5$ Oe). At low H_{ac} ($\leqslant$1 Oe), rather sharp anomalies appear at 84 K on the χ'' versus T curves, and there is a sharp drop of χ'' below 15 K with a small maximum at 5 K. Almost no difference is observed between the χ' versus T curves measured at $H_{ac} = 0.05$ and 0.25 Oe, and small differences are seen on the χ'' versus T curves at these H_{ac}. Therefore, in further measurements on $BiMnO_3$, we used $H_{ac} = 0.25$ Oe to increase the sensitivity.

Figure 2 demonstrates the temperature variations of χ' and χ'' at different ac magnetic field frequencies and $H_{ac} = 0.25$ Oe. There is a weak dependence of χ' on frequency. On the other hand, there is a strong frequency dependence of χ''. The peak near T_C on the χ'' versus T curves is suppressed with increasing frequency, and negative χ'' values are observed for $f = 1000$ Hz. This fact may indicate that the high-frequency ac field cannot alter the domain structure, resulting in the strong decrease of magnetic losses. The positions of the anomalies near 84 and 15 K are frequency-dependent.

We also studied the dependence of χ' and χ'' on different applied dc magnetic fields (at $H_{ac} = 0.25$ Oe, $f = 0.5$ and 300 Hz, on cooling from 200 to 2 K for each H_{dc}). At $H_{dc} \geqslant 1$ kOe, no frequency dependence is observed on the χ' versus T curves. The H_{dc} suppresses the sharp χ' anomalies

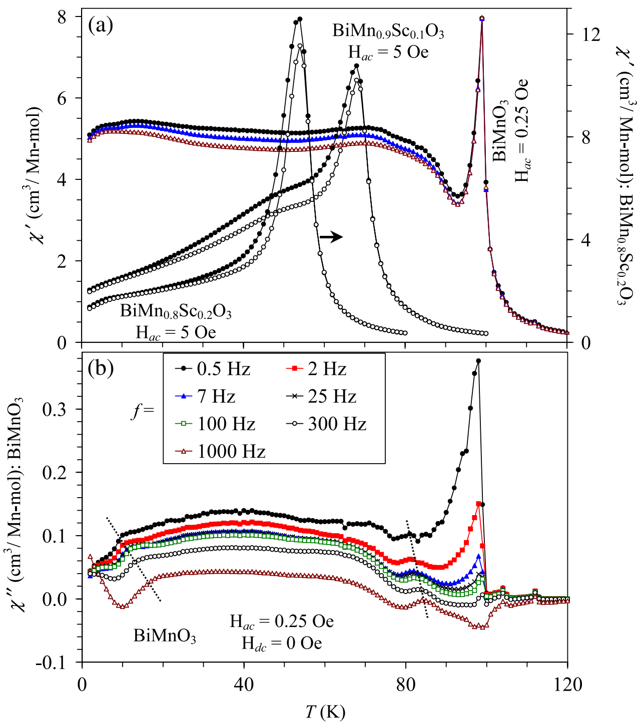

Figure 2. The real χ' (a) and imaginary χ'' (b) parts of the ac susceptibilities for $BiMnO_3$ as a function of temperature at zero static magnetic field (H_{dc}), the driving ac field (H_{ac}) of 0.25 Oe, and different frequencies. The χ' versus T curves of $BiMn_{0.9}Sc_{0.1}O_3$ and $BiMn_{0.8}Sc_{0.2}O_3$ measured at $H_{ac} = 5$ Oe and $f = 0.5$ and 300 Hz are shown in (a) for comparison.

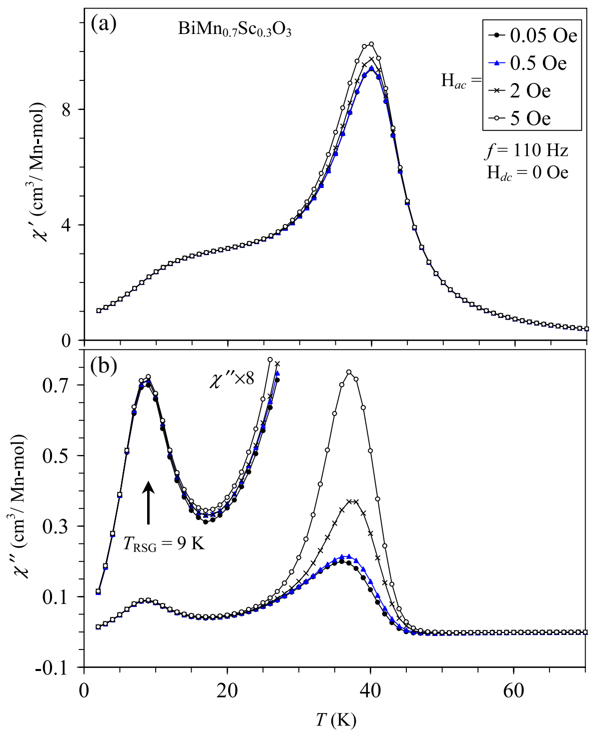

Figure 3. The real χ' (a) and imaginary χ'' (b) parts of the ac susceptibilities for $BiMn_{0.7}Sc_{0.3}O_3$ as a function of temperature at $f = 110$ Hz, $H_{dc} = 0$ Oe, and different driving ac fields (H_{ac}). The inset in (b) gives the enlarged fragment of the curves; the vertical arrow is attached to the anomalies due to the re-entrant spin-glass transition.

near T_C. Small anomalies observed on the χ'' versus T curves at 104 and 112 K are completely suppressed at $H_{dc} \geqslant 100$ Oe, and the χ'' anomalies at 84 K and $T_C = 99$ K are suppressed at $H_{dc} \geqslant 1$ kOe.

3.2. $BiMn_{1-x}Sc_xO_3$ with $x = 0.1, 0.2$, and 0.3

Figures 3 and 4 show the χ' versus T and χ'' versus T curves of $BiMn_{0.7}Sc_{0.3}O_3$ measured at different H_{ac} and f. The peak intensities of both χ' versus T and χ'' versus T are suppressed and the peak positions are shifted to higher temperatures with increasing frequency at $H_{ac} = 5$ Oe (figures 4(a), (b)). Similar behavior is observed in $BiMn_{0.9}Sc_{0.1}O_3$ and $BiMn_{0.8}Sc_{0.2}O_3$. This behavior is not consistent with the behavior of a typical SG even the peak positions shift in the right direction with frequency. In an SG, the peak intensity of χ'' versus T increases with increasing frequency [21]. At rather low H_{ac} ($H_{ac} \leqslant 0.5$ Oe), there is no dependence of χ' and χ'' on H_{ac} (figure 3), that is, we have a linear response where the inherent dynamics of a magnetic phase can be studied. As a result, at $H_{ac} = 0.01$ Oe, the peak positions of χ' and χ'' are almost independent of frequency, and the peak intensities are almost constant for $f = 2$–300 Hz (figure 4(c)). In other words, there are no SG features. In $BiMn_{1-x}Sc_xO_3$ with $x = 0.1, 0.2$, and 0.3, there is still a noticeable dependence of the χ'' values on H_{ac} near T_C (figure 3) indicating that the domain structure is established.

The enlarge sections of figures 3 and 4 demonstrate that pronounced second downward deviations in χ' versus T and corresponding maxima in χ'' versus T occur in $BiMn_{1-x}Sc_xO_3$ with $x = 0.1, 0.2$, and 0.3. These anomalies are independent of H_{ac}. For these anomalies, the peak intensities of the χ'' versus T curves increase and the peak positions shift to higher temperatures with increasing frequency at both $H_{ac} = 0.01$ and 5 Oe. These are the clear signatures of the re-entrant spin-glass (RSG) transitions [21, 22]. The RSG transition temperature (defined by the peak position on the χ'' versus T curves: $T_{RSG} = 4$, 5, and 9 K for $x = 0.1, 0.2$, and 0.3, respectively) and the intensity of the χ'' anomalies increase with increasing x in $BiMn_{1-x}Sc_xO_3$.

3.3. $BiMn_{1-x}Sc_xO_3$ with $x = 0.4, 0.5$, and 0.7

In $BiMn_{1-x}Sc_xO_3$ with $x = 0.4, 0.5$, and 0.7, no dependence of both χ' and χ'' on H_{ac} is observed between 0.01 and 5 Oe. There is only one broad anomaly on both χ' versus T and χ'' versus T curves (figure 5). The peak intensity of χ' versus T is suppressed and the peak position is shifted to higher temperatures with increasing frequency. The peak intensity of χ'' versus T increases and the peak position is shifted to higher temperatures with increasing frequency. All the above features are typical for classical SGs [21]. In SGs, a criterion, $\delta T_f = \Delta T_f/(T_f \Delta \log_{10} f)$, has often been used for comparing the frequency dependence of the spin freezing temperature T_f [21]. At $f = 0.5$ Hz, $T_f = 23.88(4)$, 17.60(3), and

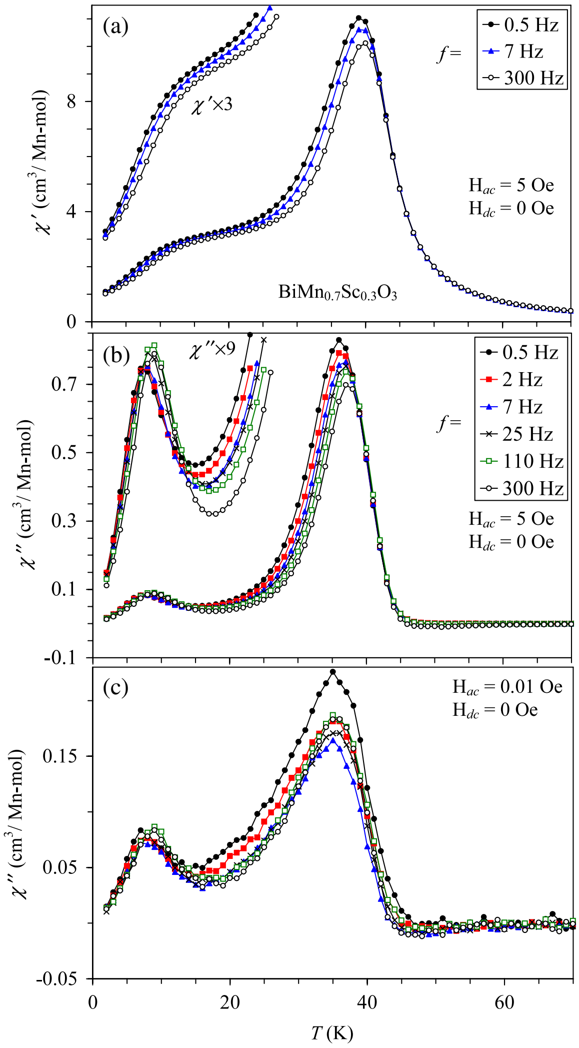

Figure 4. The real χ' (a) and imaginary χ'' (b) parts of the ac susceptibilities for $BiMn_{0.7}Sc_{0.3}O_3$ as a function of temperature at $H_{ac} = 5$ Oe, $H_{dc} = 0$ Oe, and different frequencies. The insets give the enlarged fragments of the curves. (c) χ'' versus T curves at $H_{ac} = 0.01$ Oe; for frequency values see (b).

6.74(2) K for $x = 0.4$, 0.5, and 0.7, respectively. At $f = 299.5$ Hz, $T_f = 24.54(2)$, 18.26(3), and 7.47(2) K for $x = 0.4$, 0.5, and 0.7, respectively. These data give $\delta T_f = 0.010$, 0.014, and 0.039 for $x = 0.4$, 0.5, and 0.7, respectively. These values are comparable with those reported for some spin glasses ($\delta T_f = 0.005$–0.06; see table 3.1 in [21]). We assumed variation of χ' to the Gaussian function near T_f to determine T_f; this is the reason for the apparently accurate determination of T_f. The frequency dependence of T_f is also analyzed by the empirical Vogel–Fulcher law, a well known testing equation for the SG phenomenon [21]

$$f = f_0 \exp[-E_a/k_B(T_f - T_0)] \quad (1)$$

where E_a is activation energy, k_B is the Boltzmann constant, f_0 is characteristic frequency, and T_0 is a Vogel–Fulcher temperature (a phenomenological parameter which describes the inter-particle interactions). With $f_0 = 10^{12}$ Hz typical in SG systems, we obtain good linear fits (the inset of figure 5(b))

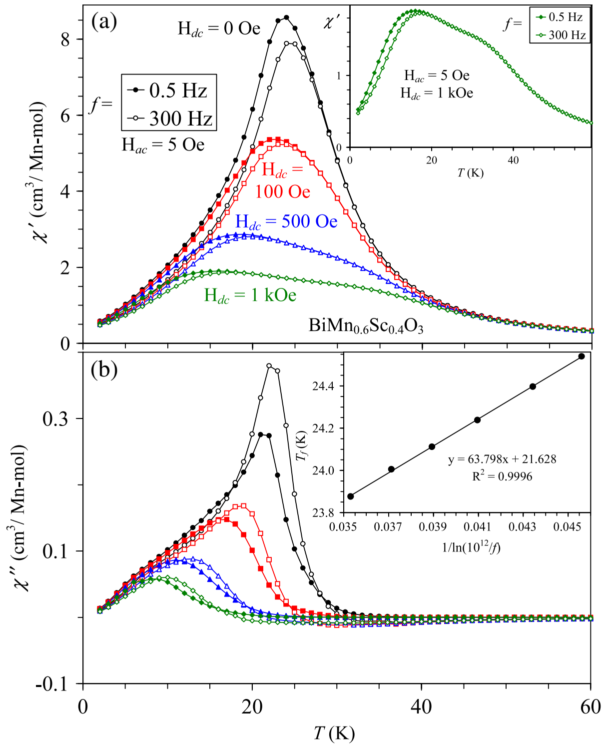

Figure 5. The real χ' (a) and imaginary χ'' (b) parts of the ac susceptibilities for $BiMn_{0.6}Sc_{0.4}O_3$ as a function of temperature at $H_{ac} = 5$ Oe, $f = 0.5$ Hz (full symbols), and 300 Hz (white symbols) and different H_{dc}. The inset in (a) shows the χ' versus T curves at $H_{ac} = 5$ Oe, $H_{dc} = 1$ kOe, and $f = 0.5$ Hz (full diamonds) and 300 Hz (white diamonds). The inset in (b) shows the fit to the Vogel–Fulcher law for the data measured at $H_{dc} = 0$ Oe.

and reasonable fitting parameters $T_0 = 21.63(3)$, 15.31(4), and 4.22(2) K and $E_a/k_B = 63.8(6)$, 64.8(9), and 71.3(4) K for $x = 0.4$, 0.5, and 0.7, respectively. Activation energy increases with x.

The dc magnetic field in $BiMn_{0.6}Sc_{0.4}O_3$ (figure 5) has the effects typical for SGs [23]. First, there is suppression of both χ' and χ'' with increasing H_{dc}. Second, there is shift of the broad maxima to lower temperatures. Third, the behavior observed at $H_{dc} = 0$ Oe is kept, that is, the peak positions are shifted to higher temperatures with increasing frequency; the peak intensity of χ' versus T is suppressed and the peak intensity of χ'' versus T is increased with increasing frequency. Fourth, at temperatures well below T_f and of course well above T_f, both components of the ac susceptibilities are almost independent of the applied dc field. This behavior is in contrast with the strong H_{dc} dependence of ac susceptibilities in $BiMnO_3$ below T_C.

We have probed the magnetic relaxation behavior for the $BiMn_{0.6}Sc_{0.4}O_3$ sample showing classical SG properties. The very large relaxation (about 30%) is observed in $BiMn_{0.6}Sc_{0.4}O_3$ at 10 K (figure 6). The relaxation significantly reduces at 20 K (about 1.2%), and almost no relaxation is observed above $T_f = 24$ K (at 30 and 40 K). Above about 10^2 s, the relaxation follows the logarithmic law typical for SGs. A strong wait-time (t_w) dependence of the magnetization is observed, and the relaxation rate ($dM/d\log_{10} t$) shows maxima

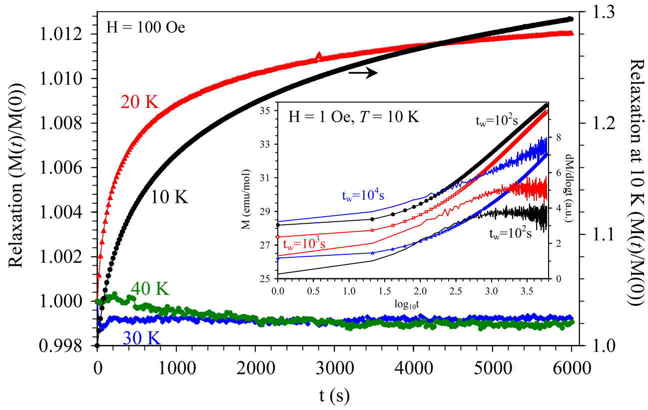

Figure 6. The relative change of magnetization ($M(t)/M(0)$) as a function of time (relaxation) in $BiMn_{0.6}Sc_{0.4}O_3$. The curves were measured at 100 Oe after cooling the sample from 150 K to the desired temperature at zero magnetic field. The inset shows the time dependence of magnetization (M) and relaxation rate ($dM/d\log_{10}t$) for the wait-time $t_w = 10^2$, 10^3, and 10^4 s; the curves were measured at 1 Oe after cooling the sample from 150 K to 10 K at zero magnetic field; the $dM/d\log_{10}t$ versus t curves were shifted for clarity.

at different times depending on t_w (the inset of figure 6). Similar aging properties are typical for SGs [22, 24].

4. Discussion

Based on the obtained results, the low-temperature phase diagram of the $BiMn_{1-x}Sc_xO_3$ system could be clarified (figure 7). After the sudden drop of T_C in $BiMn_{0.9}Sc_{0.1}O_3$ compared with that of $BiMnO_3$ due to the suppression of orbital order, T_C decreases linearly with the composition, extrapolating to zero at $x = 0.6$. However, at $x \geqslant 0.4$, a classical spin-glass transition takes place again with the almost linear compositional dependence of T_f, extrapolating to zero at $x = 0.85$.

In $BiMn_{1-x}Sc_xO_3$ with $x = 0.1$, 0.2, and 0.3, the RSG phases emerge at low temperatures, supporting the idea that at higher temperatures, ferromagnetic clusters may develop [19]. These clusters may serve as the building blocks out of which the spin-glass state is established. In the literature, it was suggested that in the presence of an RSG phase, the ferromagnetic phase may be very different from an ideal classical ferromagnetic phase with long-range order [24, 25].

The magnetic interactions in $BiMnO_3$ are partially frustrated, as already discussed in a number of works [5, 6, 16, 17], due to the presence of four ferromagnetic and two antiferromagnetic interactions. The overall magnetic structure of $BiMnO_3$ below T_C is ferromagnetic because strong ferromagnetic interactions dominate. The introduction of non-magnetic ions into the Mn-sublattice first destroys the orbital order and, therefore, weakens the magnetic interactions [19, 20]. The second effect seems to be the increase of magnetic frustration. From a certain doping concentration ($x = 0.4$), the competition between ferromagnetic and antiferromagnetic interactions produces a spin-glass state instead of long-range order. Therefore, two necessary conditions (frustration and partial randomness)

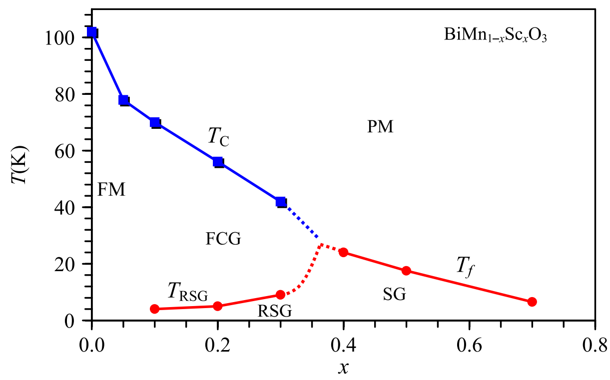

Figure 7. Low-temperature phase diagram of $BiMn_{1-x}Sc_xO_3$. T_C is the Curie temperature of ferromagnetic (FM) transition and ferromagnetic cluster–glass (FCG) transition defined by the peak position on the $d\chi/dT$ versus T curve [19]. T_f is the spin-glass (SG) freezing temperature, and T_{RSG} is the temperature of the re-entrant spin-glass (RSG) transition.

for the formation of a spin-glass state are realized in $BiMn_{1-x}Sc_xO_3$.

The appearance of spin-glass states was reported in the $LaMn_{1-x}Ga_xO_3$ system with $x = 0.35$ and 0.5 [26] and in the $LaMn_{1-x}Sc_xO_3$ system for $x = 0.28$–0.75 [27], that is, in similar compositional ranges as our $BiMn_{1-x}Sc_xO_3$ system. However, based on neutron powder diffraction, another work has reported that a long-range ferromagnetic order takes place in rather diluted samples in the $LaMn_{1-x}Ga_xO_3$ system with $x = 0.5$ and 0.6 [28]. Neutron diffraction studies of $BiMn_{1-x}Sc_xO_3$ are also very desirable.

In conclusion, we have found for the first time that re-entrant spin-glass phases emerge in the slightly doped $BiMn_{1-x}Sc_xO_3$ samples with $x = 0.1$, 0.2, and 0.3 at low temperatures. This finding shows that re-entrant spin-glass transitions may be overlooked in $LaMn_{1-x}M_xO_3$ systems. The appearance of the re-entrant spin-glass transition for $x = 0.1$–0.3 suggests that the spin-glass states are developed from the ferromagnetic-cluster regime. The classical spin-glass transition takes place in $BiMn_{1-x}Sc_xO_3$ with $x = 0.4$, 0.5, and 0.7.

References

[1] Ramesh R and Spaldin N A 2007 *Nat. Mater.* **6** 21
[2] Sharan A, Lettieri J, Jia Y, Tian W, Pan X, Schlom D G and Gopalan V 2004 *Phys. Rev.* B **69** 214109
[3] Son J Y, Kim B G, Kim C H and Cho J H 2004 *Appl. Phys. Lett.* **84** 4971
[4] dos Santos A M, Parashar S, Raju A R, Zhao Y S, Cheetham A K and Rao C N R 2002 *Solid State Commun.* **122** 49
[5] Belik A A, Iikubo S, Yokosawa T, Kodama K, Igawa N, Shamoto S, Azuma M, Takano M, Kimoto K, Matsui Y and Takayama-Muromachi E 2007 *J. Am. Chem. Soc.* **129** 971
[6] Montanari E, Calestani G, Righi L, Gilioli E, Bolzoni F, Knight K S and Radaelli P G 2007 *Phys. Rev.* B **75** 220101(R)
[7] Baettig P, Seshadri R and Spaldin N A 2007 *J. Am. Chem. Soc.* **129** 9854

[8] Montanari E, Righi L, Calestani G, Migliori A, Gilioli E and Bolzoni F 2005 *Chem. Mater.* **17** 1765
[9] Eerenstein W, Morrison F D, Scott J F and Mathur N D 2005 *Appl. Phys. Lett.* **87** 101906
[10] Gajek M, Bibes M, Barthelemy A, Bouzehouane K, Fusil S, Varela M, Fontcuberta J and Fert A 2005 *Phys. Rev.* B **72** 020406
[11] Gajek M, Bibes M, Fusil S, Bouzehouane K, Fontcuberta J, Barthelemy A and Fert A 2007 *Nat. Mater.* **6** 296
[12] Sugawara F, Iiida S, Syono Y and Akimoto S 1968 *J. Phys. Soc. Japan* **25** 1553
[13] Kimura T, Kawamoto S, Yamada I, Azuma M, Takano M and Tokura Y 2003 *Phys. Rev.* B **67** 180401(R)
[14] Moreira dos Santos A, Cheetham A K, Atou T, Syono Y, Yamaguchi Y, Ohoyama K, Chiba H and Rao C N R 2002 *Phys. Rev.* B **66** 064425
[15] Yang C H, Koo J, Song C, Koo T Y, Lee K B and Jeong Y H 2006 *Phys. Rev.* B **73** 224112
[16] Yang C H, Koo T Y, Lee S H, Song C, Lee K B and Jeong Y H 2006 *Europhys. Lett.* **74** 348
[17] Belik A A and Takayama-Muromachi E 2006 *Inorg. Chem.* **45** 10224
[18] Belik A A, Iikubo S, Kodama K, Igawa N, Shamoto S, Maie M, Nagai T, Matsui Y, Stefanovich S Yu, Lazoryak B I and Takayama-Muromachi E 2006 *J. Am. Chem. Soc.* **128** 706
[19] Belik A A, Yokosawa T, Kimoto K, Matsui Y and Takayama-Muromachi E 2007 *Chem. Mater.* **19** 1679
[20] Belik A A and Takayama-Muromachi E 2007 *Inorg. Chem.* **46** 5585
[21] Mydosh J A 1993 *Spin Glasses: An Experimental Introduction* (London: Taylor and Francis)
[22] Jonason K, Mattsson J and Nordblad P 1996 *Phys. Rev.* B **53** 6507
[23] Mattsson J, Jonsson T, Nordblad P, Aruga Katori H and Ito A 1995 *Phys. Rev. Lett.* **74** 4305
[24] Jonason K, Mattsson J and Nordblad P 1996 *Phys. Rev. Lett.* **77** 2562
[25] Suzuki I S and Suzuki M 2006 *Phys. Rev.* B **73** 094448
[26] Zhou J S, Yin H Q and Goodenough J B 2001 *Phys. Rev.* B **63** 184423
[27] Goodenough J B, Dass R I and Zhou J S 2002 *Solid State Sci.* **4** 297
[28] Blasco J, Garcia J, Campo J, Sanchez M C and Subias G 2002 *Phys. Rev.* B **66** 174431